CILAMCE 2017
Florianópolis - Santa Catarina - Brazil

COMPARISON OF THE SATELLITE ATTITUDE CONTROL SYSTEM DESIGN USING THE H∞ METHOD AND H∞/LMI WITH POLE ALLOCATION CONSIDERING THE PARAMETRIC UNCERTAINTY

Alain Giacobini de Souza[1]

Luiz Carlos Gadelha de Souza[1,2]

[1]alain.souza@outlook.com.br

[2]lcgs@unb.br

[1]National Institute for Space Research – INPE /DMC

Av. dos Astronautas, 1758 – São José dos Campos, SP – 12227-010, Brasil.

[2]Federal University of ABC – UFABC

Avenida dos Estados, 5001, Santo André, 09210-580, São Paulo-Brasil

Abstract. *This paper presents the comparison of the Attitude Control System (ACS) design for a rigid-flexible satellite with two vibrations mode, using the traditional H-infinity method and the H∞/LMI with pole allocation considering the parametric uncertainty. In the ACS design is important take into account the influence of the structure's flexibility, since they can interact with the satellite rigid motion, mainly, during translational and/or rotational maneuver, damaging the ACS. Usually the mathematic model obtained from the linearization and/or reduction of the rigid flexible model loses information about the flexible dynamical behavior and introduces some uncertainty. The satellite model is represented by a flexible beam connected to a central rigid hub considering a set of parametric uncertainties. Simulations results have shown that the control law designed by the H∞/LMI method has better performance and it is more robust than Hoo method since the first was able to support the action of the uncertainty perturbation and to control the rigid flexible satellite attitude and suppressing vibrations.*

Keywords: *H∞/LMI, Attitude Control System (ACS), parametric uncertainty*

1 INTRODUCTION

Satellites are design with specific functions and for accomplish them; the system need be able to execute some maneuvers around his center of mass (attitude maneuvers). These functions are: turning the solar panels facing the sun, stabilize the satellite after the orbital acquisition, point the cameras and/or sensors to the Earth or other planet, moon and star (Sidi, 1997). For conducting this kind of maneuver is necessary have a lot of sensors and actuators with a good accuracy and precision. With that, for managerial all that, one need design a control system called attitude control system (ACS).

The flexible appendages play an important role in the satellites ACS performance, one example of this flexible appendages are the solar arrays (Souza and Souza, 2017). Thus the dynamic of these flexible structures have to be included in the ACS design in order to investigate how its vibrational motion can affects the satellite rigid motion during translational and/or rotational maneuver which can result in damaging the ACS pointing accuracy (Souza and Souza, 2015).

Another problem is to recovery the loss of the dynamics information associated with the inability to obtain the real model, since the model reduction (Pinheiro and Souza, 2014) can introduced some kind of perturbation which can be represented by the parametric and non parametric uncertainties where the first is associated with the parameters variation and the second with the unmodelled dynamics (unstructured uncertainty).

Than to obtain a ACS one applies the H_∞ control method, since this method has the property to incorporate the uncertainties in its formulation (Gasbarri et al., 2014), and suppress the loss of the dynamics information. Other technic used is the H_∞ control method subject a pole allocation using Linear Matrix Inequalities.

The ACS design consider a model of a satellite with one panel, like the China Brazil Earth Resources Satellite – CBERS (Fig. 1), making an attitude acquisition around the axis here the system are more flexible, this kind of maneuver can be modeled (Junkins, 1993), by an analogous as a flexible rotatory beam.

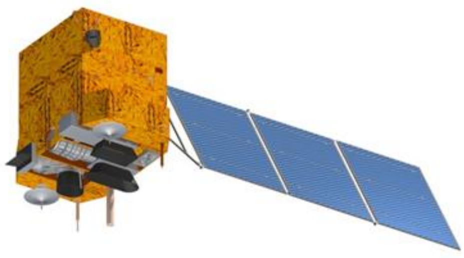

Figure 1. China Brazil Earth Resources Satellite – CBERS

The main point of the paper consists in study comparatively the performance and robustness of the H_∞ method with the technic that join the H_∞ method with a LMI pole allocation, applied to a flexible structure that simulates a critical attitude maneuver with a parametrical uncertainty associate to the mass matrix. Those studies led to development of software capable of check the performance of de ACS design with a H_∞ or H_∞ with a LMI pole allocation subjects some requirements for select the best controller, for a phase A of a project.

2 ROBUST CONTROLLER DESIGN

For this problem it was design two controls law, one using a H_∞ control method and other using the technic H_∞ method with LMI pole allocation. The procedures used for this design are developed in sequence.

2.1 H_∞ control method with parametric uncertainty

The H infinity control method have the advantage to inserts structured uncertainty and/or unstructured uncertainty in the design of the controller (Zhou, 1998). The philosophy behind the control method is to found a gain $\mathbf{K}_{H\infty}$ that minimizing the H infinity norm of the closed loop function (Eq. (1)) in a system subject a generalized plant model **P**,

$$\boldsymbol{F_l(P, K_{H\infty})\omega = P_{11} + P_{12}K_{H\infty}(I - P_{22}K_{H\infty})^{-1}P_{21}} \tag{1}$$

$$\boldsymbol{\left|\left|F_l(P, K_{H\infty})\right|\right|_\infty = max_\omega\, \bar{\sigma}\left(F_l(P, K_{H\infty})(j\omega)\right);\ \ \left|\left|F_l(P, K_{H\infty})\right|\right|_\infty < \gamma} \tag{2}$$

where $F_l(\mathbf{P}, \mathbf{K}_{H\infty})$ is the linear fractional transformation (LFT) of **P** and $K_{H\infty}$, and the γ is a design parameter which the smallest value is associated with the space state realization, such that the Hamiltonian **H** (Eq.(3)) has no eigenvalues on the imaginary axis (Skogestad, 2001),

$$\boldsymbol{H = \begin{bmatrix} A + BR^{-1}D^TC & BR^{-1}B^T \\ -C^T(I + DR^{-1}D^T)C & -(A + BR^{-1}D^TC)^T \end{bmatrix}} \tag{3}$$

Proceedings of the XXXVIII Iberian Latin-American Congress on Computational Methods in Engineering
P.O. Faria, R.H. Lopez, L.F.F. Miguel, W.J.S. Gomes, M. Noronha (Editores), ABMEC, Florianópolis, SC, Brazil, November 5-8, 2017.

where **A**, **B**, **C** and **D** are the space state matrices and $\mathbf{R} = \gamma^2\mathbf{I} - \mathbf{D}^T\mathbf{D}$.

One can also include in the H-infinity solution some weight functions in the system as showed in the Fig. 2.

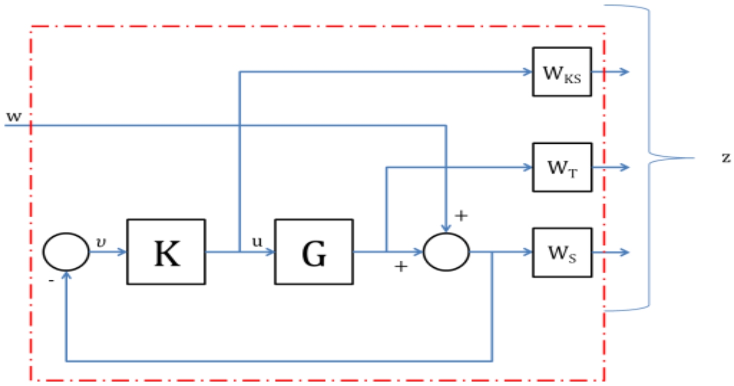

Figure 2. Tuning weight functions

Should be mentioned that in the optimization of the H infinity control method to find the gain **K** one uses the criterion of the smallest value of γ associated with the tuning weight function which have the following form (Ferreira et al., 2011):

$$\boldsymbol{W_s = \frac{\frac{s}{M}+\omega_b}{s+\omega_b A}, \quad W_T = \frac{s+\frac{\omega_{bc}}{M}}{As+\omega_{bc}}, \quad W_{KS} = cte} \qquad (4)$$

The parameters of the weight functions are: A is correlated with the steady state, ω_b is the desired bandwidth of the sensitivity function, M is correlated with the overshoot, ω_{bc} is the desired bandwidth of the complementary sensitivity function (Zhou, 1998).

2.2 H∞ method using a LMI pole allocation

For the pole allocation is necessary that the closed loop function obey the restriction $\|T\|_{wz\infty} < \gamma$ and the matrix $\mathbf{X}_\infty$ exists and $\mathbf{X}_\infty > 0$ (Wu and LI, 2009).

$$\boldsymbol{\begin{bmatrix} (A+B_2K)X_\infty + X_\infty(A+B_2K)^T & B_1 & X_\infty(C_1+D_{12}K)^T \\ B_1^T & -I & D_{11}^T \\ (C_1+D_{12}K)X_\infty & D_{11} & -\gamma^2 I \end{bmatrix} < 0} \qquad (5)$$

To guarantee the pole allocation in a LMI region defined by,

$$\boldsymbol{D = \{z \in C : L + zM + \bar{z}M^T < 0\}} \qquad (6)$$

with $\mathrm{L} = \mathrm{L}^T = [\lambda_{ij}]_{1\le i,j\le m}$ and $\mathrm{M} = \mathrm{M}^T = [\mu_{ij}]_{1\le i,j\le m}$. And is necessary, there is a matrix $\mathbf{X}_{pol} > 0$ that satisfies the relationship:

$$[\boldsymbol{\lambda_{ij} X_{pol} + \mu_{ij}(A + B_2 K) X_{pol} + \mu_{ij} X_{pol} + \mu_{ij} X_{pol}(A + B_2 K)^T_{1\le i,j\le m} < 0} \tag{7}$$

That conjunct of conditions is create a non-convex optimization with the variables **K**, $\mathbf{X}_\infty$ and $\mathbf{X}_{pol}$. For the pole allocation it's chosen the combination of three LMI regions, a plan, a half disc and a conic sector (Chilali et al, 2015) this region is represented by the Fig. 3:

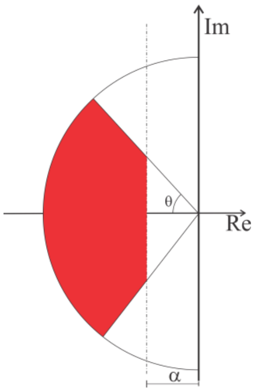

Figure 3. LMI Region

The intersection of these three regions guarantees an allocation of poles such that the transient response is: 1) decay rate equal α; 2) Natural frequency of minimum damping $\zeta = \cos(\theta)$; 3) Natural frequency undamped $D = rsin(\theta)$. This in turn limits the maximum overshoot, the frequency of vibration modes, the delay time, rise time and duration of the accommodation. Thus, the pole assignment closed loop system in that region provides a satisfactory transient response.

3 DYNAMIC MODEL WITH PARAMETRIC UNCERTAIN

The rigid-flexible satellite was modeled like a flexible rotatory beam (Bigot and Souza, 2013). The actuator is located in the central part, and it is responsible for the control of the horizontal planar movement of the rigid structure and by the elastic displacement, where (X_0, Y_0) and (X, Y) are the coordinates system before and after deformation, respectively. The rigid central hub has radius R, the actuator rotor has viscous friction b_m, and inertia J_{ROTOR} and develops a torque $\tau(t)$; the flexible beam has uniform linear mass density ρ, uniform bending stiffness EI and length L; the flexible beam deformation is $w(x, t)$; and the tip mass is m_{tip} and inertia J_{tip}; $\alpha(t)$ represent the tip angle and $\theta(t)$ is the rigid angle displacement; and $s(x)$ represent the distance between the referential axis to an element of mass in the link.

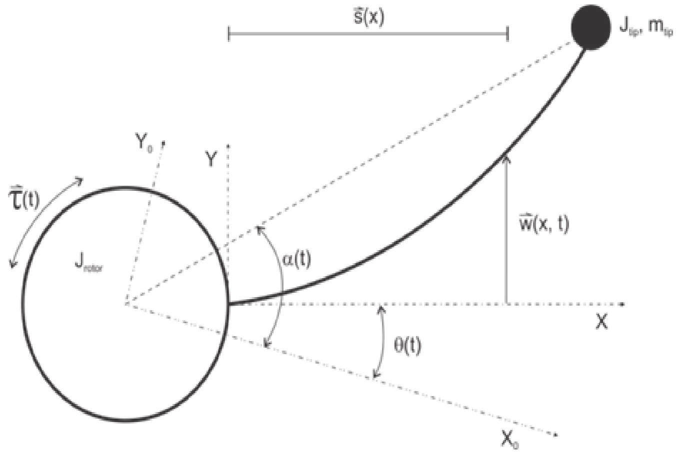

Figure 4. Satellite Analogous Representation

The flexible link is considered an Euler-Bernoulli beam. The equations of motion are derived using the Lagrangian approach combined with the assumed modes method, admitting two vibrations mode. The flexible link is considered an Euler-Bernoulli beam. Like show in (Souza and Souza, 2015) the equations of the motion was derived using a Lagrangian approach combined with the assumed modes methods, admitting two vibrations modes and a dissipation of energy in a Rayleigh form (Souza and Souza, 2015). Then the equations linearized of the dynamics are represented in a matrix form:

$$\begin{bmatrix} \boldsymbol{I_t} & \boldsymbol{M_{rf}^T} \\ \boldsymbol{M_{rf}} & \boldsymbol{M_{ff}} \end{bmatrix} \begin{bmatrix} \boldsymbol{\theta} \\ \boldsymbol{\ddot{q}} \end{bmatrix} + \begin{bmatrix} \boldsymbol{b_m} & \boldsymbol{0} \\ \boldsymbol{0} & \boldsymbol{B_{ff}} \end{bmatrix} \begin{bmatrix} \boldsymbol{\dot{\theta}} \\ \boldsymbol{\dot{q}} \end{bmatrix} + \begin{bmatrix} \boldsymbol{0} & \boldsymbol{0} \\ \boldsymbol{0} & \boldsymbol{K_{ff}} \end{bmatrix} \begin{bmatrix} \boldsymbol{\theta} \\ \boldsymbol{q} \end{bmatrix} = \begin{bmatrix} \boldsymbol{\tau} \\ \boldsymbol{0} \end{bmatrix} \tag{8}$$

With,

$$\begin{aligned}
&\boldsymbol{B_{ff}} = \boldsymbol{k_e EI} \int_0^L \boldsymbol{\phi''\phi''^T dx}\\
&\boldsymbol{K_{ff}} = \boldsymbol{EI} \int_0^L \boldsymbol{\phi''\phi''^T dx}\\
&\boldsymbol{K_{ff}} = \boldsymbol{EI} \int_0^L \boldsymbol{\phi''\phi''^T dx}\\
&\boldsymbol{M_{ff}} = \boldsymbol{\rho} \int_0^L \boldsymbol{\phi\phi^T dx} + \boldsymbol{m_{tip}\phi_L\phi_L^T} + \tfrac{1}{2}\boldsymbol{J_{tip}\phi'_L\phi'^T_L}
\end{aligned} \tag{9}$$

where $\theta$is the rigid angular displacement, $\mathbf{q}$ the flexible displacement vector and $\boldsymbol{\phi}$ is the function of the modal form. By analogies, the Eq. (8) represent the standard form $\mathbf{M}\ddot{x} + \mathbf{D}\dot{x} + \mathbf{K}x = \mathbf{Q}u$, where the matrix are called $\mathbf{M}$ is the mass matrix, $\mathbf{D}$ is the damping matrix and $\mathbf{K}$ is the rigid matrix. Writing the space state form, one has

$$\begin{bmatrix}\dot{\boldsymbol{X}}_1\\ \dot{\boldsymbol{X}}_2\end{bmatrix} = \begin{bmatrix}\mathbf{0} & \boldsymbol{I}\\ -\boldsymbol{M^{-1}K} & -\boldsymbol{M^{-1}D}\end{bmatrix}\begin{bmatrix}\boldsymbol{X_1}\\ \boldsymbol{X_2}\end{bmatrix} + \begin{bmatrix}\mathbf{0}\\ \boldsymbol{M^{-1}Q}\end{bmatrix}\boldsymbol{u} \tag{10}$$

with $\mathbf{X}_1 = \theta$ and $\mathbf{X}_2 = \mathbf{q} = [q_1 \quad q_2]$ is the state's vectors and the control $\mathbf{u} = -\mathbf{K}_{H_\infty}\boldsymbol{X}$, where $\mathbf{K}_{H_\infty}$ is the gain calculate by the H infinity method [3].

3.1 Uncertainty design

The uncertainty of the mass matrix ($\mathbf{M}$) can be introduced re-writing Eq.(10) in the follow form:

$$\begin{bmatrix}\dot{\mathbf{X}}_1\\ \dot{\mathbf{X}}_2\end{bmatrix} = \begin{bmatrix}0 & \mathbf{I}\\ -\left(\boldsymbol{\bar{M}}(\boldsymbol{I} + \boldsymbol{p_m^{-1}\delta_m})\right)^{-1}\mathbf{K} & -\left(\boldsymbol{\bar{M}}(\boldsymbol{I} + \boldsymbol{p_m^{-1}\delta_m})\right)^{-1^{-1}}\mathbf{D}\end{bmatrix}\begin{bmatrix}\mathbf{X}_1\\ \mathbf{X}_2\end{bmatrix} + \begin{bmatrix}\mathbf{0}\\ (\boldsymbol{\bar{M}}(\boldsymbol{I} + \boldsymbol{p_m^{-1}\delta_m}))^{-1}\boldsymbol{Q}\end{bmatrix}\boldsymbol{u} \tag{11}$$

where $\bar{\mathbf{M}}$ is the mass nominal value, p_m is the uncertain values and $\boldsymbol{\delta}_m$ is the amplitude of the uncertain ($-1 \leq \boldsymbol{\delta}_\mathrm{m} \leq 1$). The matrix $\bar{\mathbf{M}}^{-1}$ can be represented by a linear fraction transformation (LFT) in δ_m , like:

$$\boldsymbol{\bar{M}^{-1}} = \boldsymbol{\bar{M}^{-1}}(\boldsymbol{I} + \boldsymbol{p_m\delta_m})^{-1} = \boldsymbol{F_U}(\boldsymbol{M_{mi}}, \boldsymbol{\delta_m}) \tag{12}$$

The block diagram of the Fig. 4 shows how the uncertainty acts as a perturbation in the system interconnections.

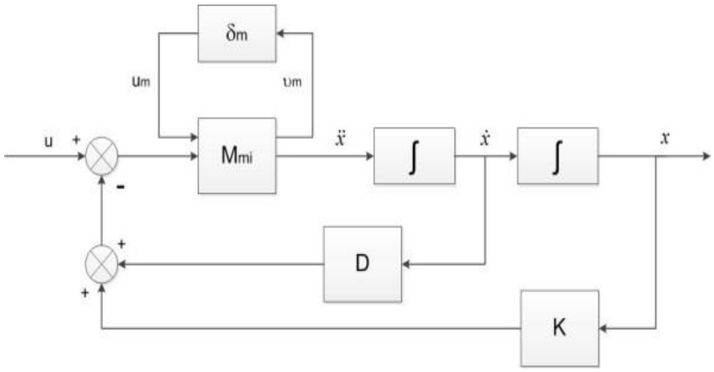

Figure 5. Block diagram of the system with uncertainty

The uncertain in this problem actuate in the matrices **M**. Than the uncertain amplitude is given by $\boldsymbol{\delta}_m$. One have 27 possibilities of $\boldsymbol{\delta}_m$, or else, we have 27 cases of uncertainties for each matrix **M.**

4 SIMULATIOS RESULTS

The objective of the control simulation is stabilizing the tip angle (α) of the flexible link in a neutral position (0°).

$$\boldsymbol{\alpha(t) = arctan\left(\frac{w(x,t)}{L+R}\right) + \theta} \tag{13}$$

When the tip comes to the neutral positions is important to see if the vibration was suppress, because with that we can assure that the control law design was robust enough to absorb the uncertainties.

For the simulation the constant parameter are: R= 0.05 m, bm= 0.15 m2/s, Jrotor= 0.3kgm2, L= 1 m, ρ= 2700 kg/m, ke= 0.03, EI= 18.4 Nm2, mtip= 0.25 kg and Jtip=0.04kgm2. One applies the H infinity control method for the 27 possible cases of uncertainty and the H_∞ controller gain for every case of uncertainty must be robust enough to control the flexible link in a time interval of 200 s and an initial condition $\theta = 1^o$.

4.1 Using the H_∞ control method

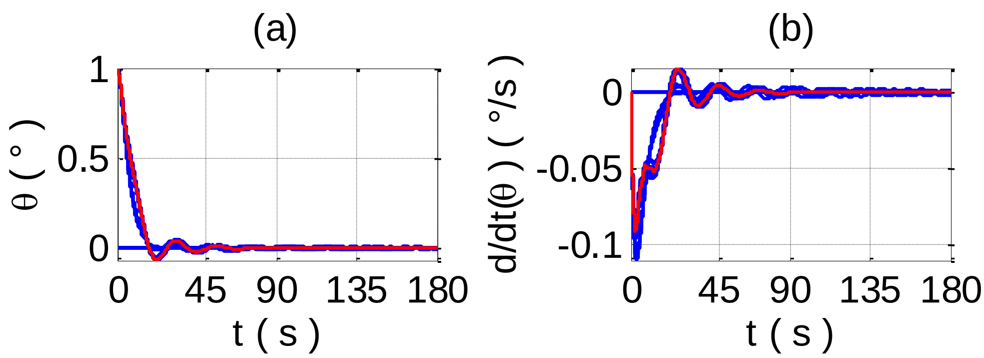

Figure 6. The angle θ and velocity $\dot{\theta}$, where red and blue lines are the nominal and the uncertainty cases

Proceedings of the XXXVIII Iberian Latin-American Congress on Computational Methods in Engineering
P.O. Faria, R.H. Lopez, L.F.F. Miguel, W.J.S. Gomes, M. Noronha (Editores), ABMEC, Florianópolis, SC, Brazil, November 5-8, 2017.

The Fig. 6 shows that H_∞ controller is able to control the rigid displacement θ (attitude) for the nominal case (red line: uncertainty zero) and for 16 cases of uncertainties (blue line) in less than 90 s. It is possible to see that some uncertainty cases the answer is better than the nominal case, showing that the influence of some parameters variation works to help the controller in the sense of minor overshoot and time rise.

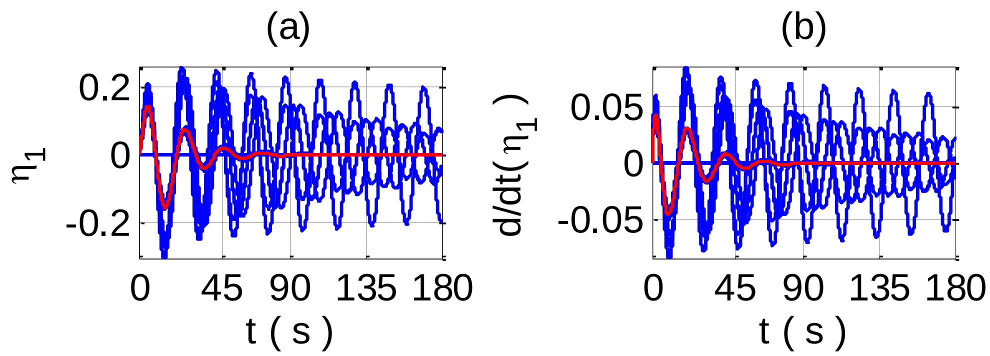

Figure 7. The flexible mode η_1 and rate $(\dot{\eta}_1)$ - red and blue lines are the nominal and the uncertainty cases.

The Fig. 7 shows that H_∞ controller is able to control the coordinate generalized of the first mode (η_1) and the variation rate of the first flexible mode $(\dot{\eta}_1)$, for the nominal case (red line: uncertainty zero) and for 16 cases of uncertainties (blue line) in less than 100 s.

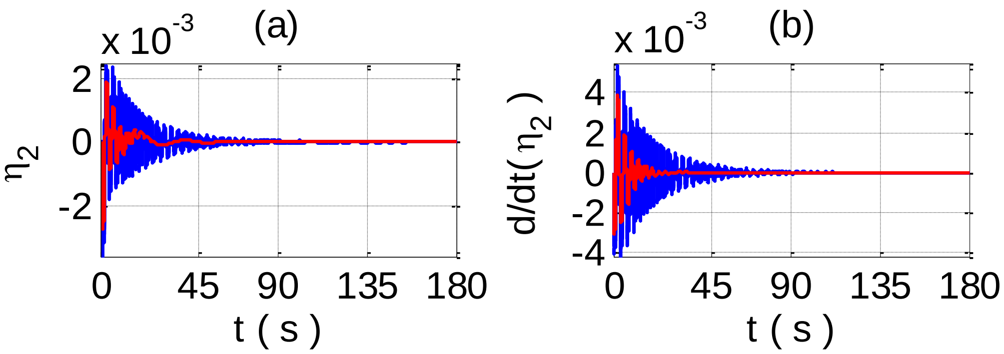

Figure 8. The flexible mode η_2 and rate $(\dot{\eta}_2)$ - red and blue lines are the nominal and the uncertainty cases.

The Fig. 8 shows that H_∞ controller is able to control the coordinate generalized of the second mode (η_2) and the variation rate of the first flexible mode ($\dot{\eta}_2$), for the nominal case (red line: uncertainty zero) and for 16 cases of uncertainties (blue line) in less than 90 s.

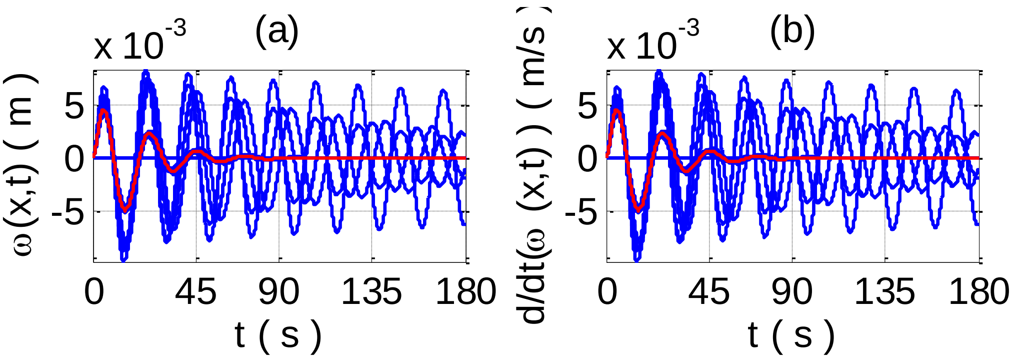

Figure 9. Comportment of the flexible displacement $\vec{w}(x,t)$ and his taxes variation.

In the Fig.9, shows the comportment of the flexible displacement $\vec{w}(x\ t)$ and his taxes variation $\dot{\vec{w}}(x,t)$, for the nominal case (red line: uncertainty zero) and for 16 cases of uncertainties (blue line), considering two vibrations modes. The maximum displacement was about 0,006 m.

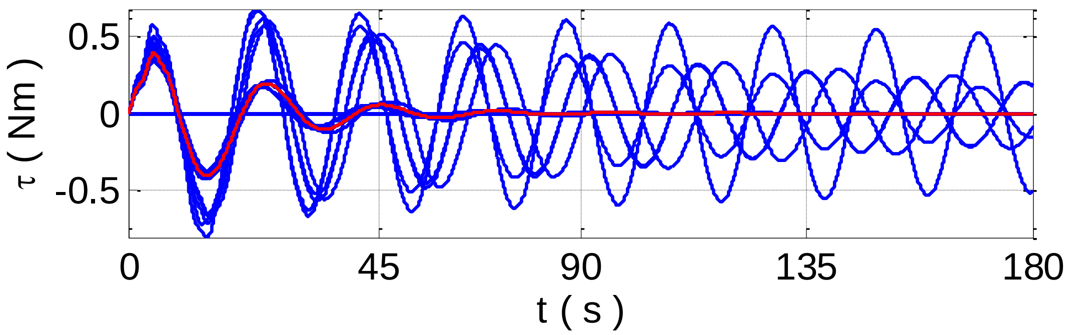

Figure 10. Response of the control effort τ, the red line is the nominal case and the blue lines are the uncertainty cases.

Figure 10 show the H-infinity Energy spend (torque τ) to control the all 27 uncertainties cases (blue lines) where the red line is the nominal case. The response of the torque action shows that for 16 cases of uncertainties the system reach the equilibrium in less than 90 s with a maximum torque of 0.6 Nm.

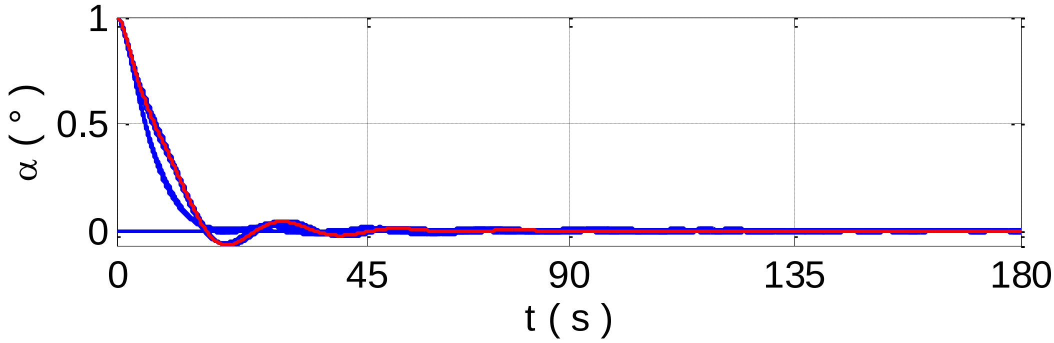

Figure 11. Response of the angular position of the tip mass α, the red line is the nominal case and the blue lines are the uncertainty cases.

Figure 11 show the angular position of the tip mass (α). The response of the evolution of the α angle shows that for 16 cases of uncertainties the system reach the equilibrium in less than 90 s. It is possible to see that some uncertainty cases the answer is better than the nominal case, showing that the influence of some parameters variation works to help the controller in the sense of minor overshoot and time rise.

For 11 cases of uncertainties the H_∞ method as not able to control, because this cases violates the boundary condition of this method.

4.2 Using the H_∞ /LMI control method

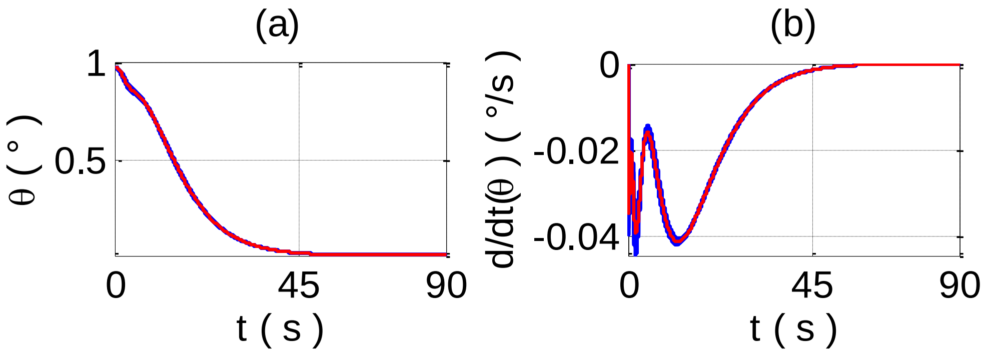

Figure 12. The angle θ and velocity $\dot{\theta}$, where red and blue lines are the nominal and the uncertainty cases

The Fig. 12 shows that H_∞ method using a LMI pole allocation is able to control the rigid displacement θ (attitude) for the nominal case (red line: uncertainty zero) and for all 27 cases of uncertainties (blue line) in less than 50 s.

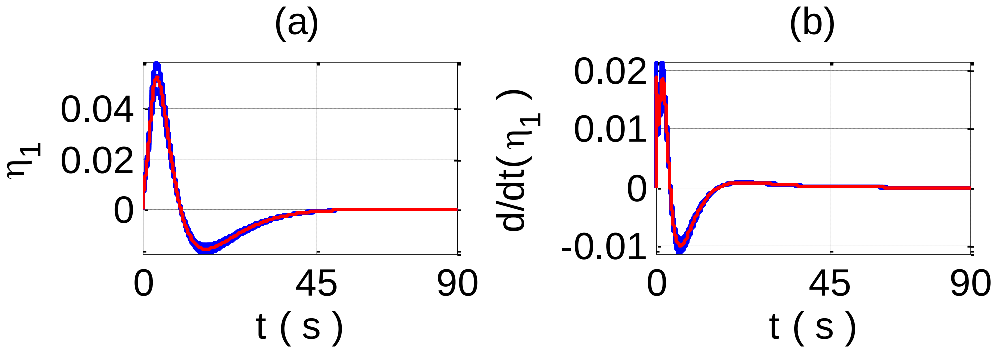

Figure 13. The flexible mode η_1 and rate ($\dot{\eta}_1$) - red and blue lines are the nominal and the uncertainty cases.

The Fig. 13 shows that H_∞ method using a LMI pole allocation is able to control the coordinate generalized of the first mode (η_1) and the variation rate of the first flexible mode ($\dot{\eta}_1$), for the nominal case (red line: uncertainty zero) and for all 27 cases of uncertainties (blue line) in less than 50 s.

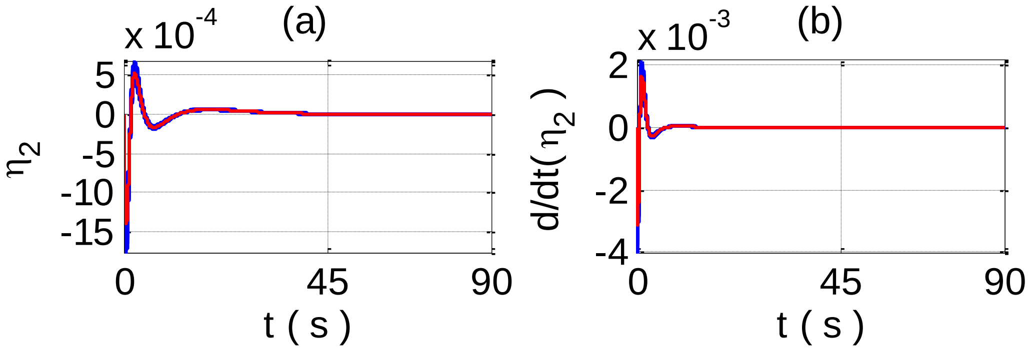

Figure 14. The flexible mode η_2 and rate ($\dot{\eta}_2$) - red and blue lines are the nominal and the uncertainty cases.

The Fig. 14 shows that H_∞ method using a LMI pole allocation is able to control the coordinate generalized of the second mode (η_2) and the variation rate of the second flexible mode ($\dot{\eta}_2$), for the nominal case (red line: uncertainty zero) and for all 27 cases of uncertainties (blue line) in less than 45 s.

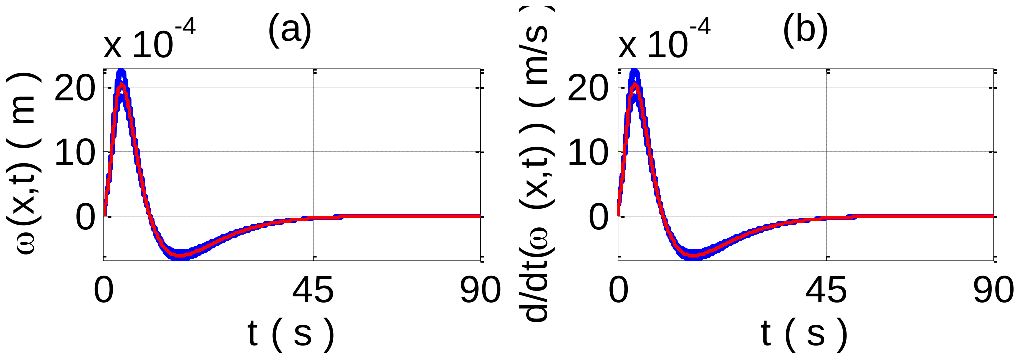

Figure 15. Comportment of the flexible deformation $\vec{w}(x,t)$ and his taxes variation.

In the Fig. 15, shows the comportment of the flexible displacement $\vec{w}(x\,t)$ and his taxes variation $\dot{\vec{w}}(x,t)$, for the nominal case (red line: uncertainty zero) and for 16 cases of uncertainties (blue line), considering two vibrations modes. The maximum displacement was about 0,006 m.

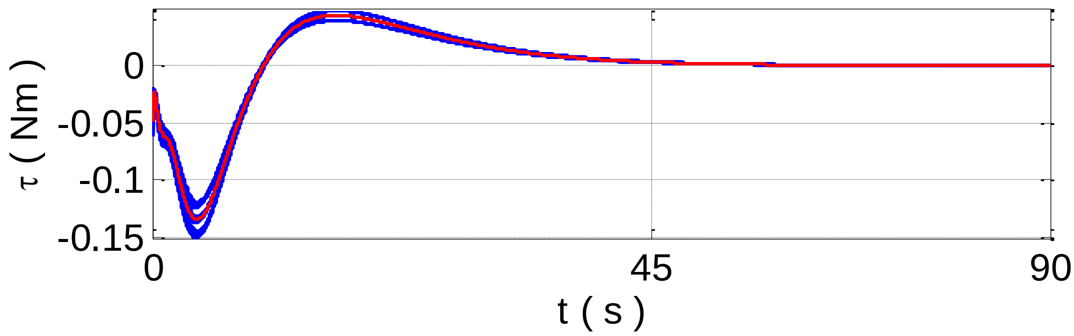

Figure 16. Response of the control effort τ, the red line is the nominal case and the blue lines are the uncertainty cases.

Figure 16 show the H_∞ Energy spend (torque τ) to control the all 27 uncertainties cases (blue lines) where the red line is the nominal case. The response of the torque action shows that for all 27 cases of uncertainties the system reach the equilibrium in less than 60 s with a maximum torque of 0.15 Nm.

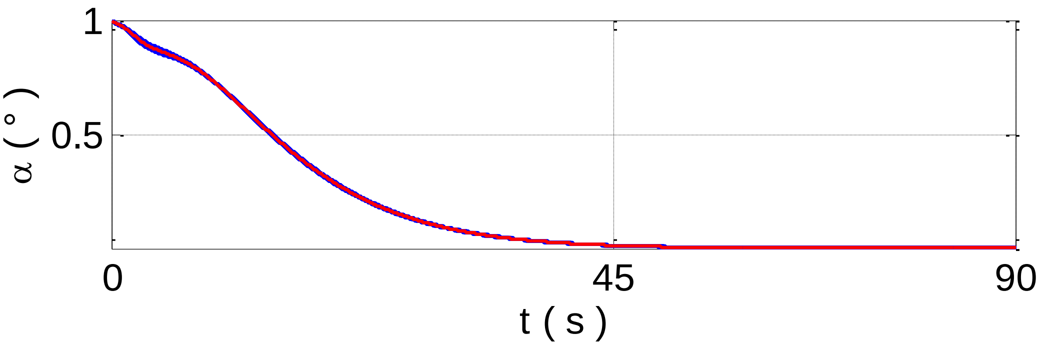

Figure 17. Response of the angular position of the tip mass α, the red line is the nominal case and the blue lines are the uncertainty cases.

Proceedings of the XXXVIII Iberian Latin-American Congress on Computational Methods in Engineering
P.O. Faria, R.H. Lopez, L.F.F. Miguel, W.J.S. Gomes, M. Noronha (Editores), ABMEC, Florianópolis, SC, Brazil, November 5-8, 2017.

Figure 17 show the angular position of the tip mass (α). The response of the evolution of the α angle shows that for all 27 cases of uncertainties the system reach the equilibrium in less than 60 s.

4.3 Comparison between the two cases

From the set of figures presented it is very explicit that the performance of the control law design with the method H_∞ with a LMI pole allocation was better, than the case were the control law was designed with only the H infinity method.

Comparing the Fig. 6 and 12 (the angle rigid (θ) and his velocity ($\dot{\theta}$)) it is verified that the variable was controlled in a shorter time (about 90 s) for the case with pole allocation (Fig. 12). The Fig. 7 and 13 (coordinate generalized of the first mode (η_1) and the variation rate of the first flexible mode ($\dot{\eta_1}$)) it is verified that the variable was controlled in a shorter time (about 50 s) for the case with pole allocation (Fig. 13). The Fig. 8 and 14 (coordinate generalized of the second mode (η_2) and the variation rate of the second flexible mode ($\dot{\eta_2}$))) it is verified that the variable was controlled in a shorter time (about 45 s) for the case with pole allocation (Fig. 14). The Fig. 9 and 15 (the angle rigid ($\vec{w}(x,t)$) and his taxes variation ($\dot{w}(x,t)$)) it can be seen that the maximum deflection generated in the case with pole allocation was lower than that obtained with the only H infinity method. The Fig. 11 and 17 (the flexible angle (α)) has the same observations that make to the rigid angle. The Fig. 10 and 16 shows the torque engenders, for the same task, the control law design with the H infinity with a LMI pole allocation was 25 % less than that provided by the other method.

And for all cases the control law design with H infinity LMI pole placement was able to control all cases of uncertainty.

5 CONCLUSIONS

This paper presents an attitude controller design for a rigid-flexible satellite comparing the performance between H_∞ method considering and H_∞ LMI pole placement with a parametrical uncertainty apply to the mass matrix.

The result of the simulations shows that the control laws designs, for the rigid flexible satellite, was able to support the parametric uncertainty and suppress the vibrations. The control law design with the H_∞ with a LMI pole allocation was 25 % less than that provided by the other method.

The controller design with the H_∞ method with LMI pole allocation is more robust than the one provided by the H_∞ method.

ACKNOWLEDGEMENTS

The authors would like to thank CAPES and INPE/DMC.

REFERENCES

Sidi, M. J, 1997. "Spacecraft dynamics and control: A practical engineering approach". New York, NY: Cambridge University Press.

Souza, S. G.; Souza, L. C. G, 2017. "Attitude Control System Design For A Rigid-Flexible Satellite Using The H-Infinity Method With Parametric Uncertainty". Revista Interdisciplinar de Pesquisa em Engenharia, v. 2, p. 1-10.

Souza, A.G, Souza, L. C. G, 2015 "H infinity controller design to a rigid-flexible satellite with two vibration modes," Journal of Physics: Conference Series, vol. 641, pp. 012030.

Pinheiro, E.R., Souza L.C.G, 2013. "Design of the Microsatellite Attitude Control System Using the Mixed $H2/H\infty$ Method via LMI Optimization," Mathematical Problems in Engineering, vol. 2013, Article ID 257193, 8 pages. doi:10.1155/2013/25719.

P. Gasbarri, R. Monti, C. De Angelis, M. Sabatini, 2014. "Effects of uncertainties and flexible dynamic contributions on the control of a spacecraft full-coupled model", Acta Astronautics, Volume 94, Issue 1, January–February 2014, Pages 515-526, ISSN 0094-5765, http://dx.doi.org/10.1016/j.actaastro.2012.08.018.

Junkins, J. L, Kim, 1993. Y. "Introduction to dynamics and control of flexible structures". Washington, DC: American Institute of Aeronautics and Astronautics (AIAA).

Zhou, K, Doyle, J. C, "Essentials of robust control". Upper Saddle River, NJ: Prentice-Hall, 1998.

Skogestad, S, Postlethwaite, I, 2001. "Multivariable feedback control: analysis and design". Chichester, UK: John Wiley and Sons.

H. C. Ferreira, R. S. Baptista, J. Y. Ishihara and G. A. Borges, 2011. "Disturbance rejection in a fixed wing UAV using nonlinear $H\infty$ state feedback," 2011 9th IEEE International Conference on Control and Automation (ICCA), Santiago, pp. 386-391.

Gu D.W., Petkov P.H., Konstantinov M.M, 2005. Robust control design, with matlab, London, UK Springer.

Chilali, M. Gahinet, P. Apkarian, 1999. "Robust pole placement in lmi regions". IEEE Transactions on automatic control, v. 44, n. 12, p. 2257 – 2270.